Thermochimica Acta, 171 (1990) 253–277
Elsevier Science Publishers B.V., Amsterdam

THERMAL PROPERTIES, CRYSTAL LATTICE ENERGY, MECHANISM AND ENERGETICS OF THE THERMAL DECOMPOSITION OF HYDROCHLORIDES OF 2-AMINO ACID ESTERS

JANUSZ RAK, JACEK ŁUBKOWSKI, IRENA NIKEL, JÓZEF PRZYBYLSKI and JERZY BŁAŻEJOWSKI

Institute of Chemistry, University of Gdańsk, 80-952 Gdańsk (Poland)

(Received 2 April 1990)

ABSTRACT

The thermal behaviour of hydrochlorides of esters (mostly methyl esters) of several naturally occurring 2-amino acids was examined by thermoanalytical methods (DTA, TG, DTG). Heating of the compounds at a constant rate up to 750 K leads to their total or partial volatilization and formation, in the latter case, of a non-volatile residue comprising a mixture of carbonization products. The thermodynamics of the thermal decomposition of the compounds studied was analysed by considering several possible pathways for primary processes. The thermochemical characteristics necessary for these considerations, such as the enthalpies of formation of gaseous 2-amino acid esters and of their crystalline hydrochlorides, were estimated on the basis of the Benson group additivity method and available literature information. Using characteristics thus derived and other data from the literature, the enthalpies of primary processes were evaluated, as well as volatilization temperatures of some of the reaction products. The MINDO/3, MNDO and AM1 quantum chemistry methods were applied to evaluate several physicochemical characteristics, in the gaseous phase, for glycine and L-alanine methyl esters and glycine ethyl ester, and also for their protonated forms and decomposition fragments. The thermodynamics of the thermal decomposition of the three above mentioned compounds was then examined using the thermochemical characteristics for gaseous reactants derived by MINDO/3, MNDO and AM1. The AM1 method was also applied to analyse structure and energetics of the transition state (saddle point structure) for the decarboxylation of glycine methyl ester. Further, the electrostatic energy of the hydrochloride of L-proline phenylmethyl ester was derived on the basis of the Ewald method and the known crystal structure of the compound. This quantity has been compared with values of crystal lattice energy of hydrochlorides of several other amino acid esters estimated on the basis of the thermochemical cycle using available literature information and the heats of formation of gaseous amino acid esters and their monocations evaluated by quantum chemistry methods.

INTRODUCTION

Incorporation of a nitrogen atom in an organic molecule gives it basic properties. This results from the presence of a lone electron pair remaining

0040-6031/90/$03.50

at this atom. Nitrogen organic bases can thus interact with molecules having a vacancy of electrons through electron donor–acceptor (EDA) interactions. In the case of strong binding, this leads to stable adduct-type derivatives. Nitrogen bases can also participate in hydrogen bond-type interactions. These interactions are very common in various biological systems. A particularly interesting case is that in which a proton from the Brønsted acid is strongly bound to nitrogen, forming a cation. Such interactions lead to salt-type derivatives. Protonation at nitrogen markedly influences the behaviour of molecules, e.g. increases their solubility in aqueous media and decreases their volatility. Protonated forms can also be involved in electrostatic interactions. This strongly influences the behaviour of organic nitrogen bases in biological systems [1,2]. The nature of the hydrogen bond in solid salt-like compounds containing nitrogen bases can be examined by thermoanalytical methods. In several previous works we have studied thermal features and thermochemistry of chloride [3–5], bromide [6], iodide [7], hexachlorostannate [8–10] and hexachloroplumbate [11] salts of mononitrogen organic bases such as alkanamines, aromatic amines and heterocyclic nitrogen bases. These compounds represent one of the simplest molecular forms of nitrogen organic bases. The very common units forming a large number of organic macromolecules are amino acids. In the pure state they form zwitterionic structures which do not exhibit basic character. The basic function of these derivatives is, however, preserved in esters of amino acids. The thermal features, other properties, thermochemistry and crystal lattice energy of hydrochlorides of these latter derivatives, as well as the mechanism and energetics of the decomposition of simple free amino acid esters, are examined in this work. Such derivatives are commonly used in organic synthesis. They also present interesting model compounds for thermoanalytical investigations due to the presence of a second functional group besides the amino group, i.e. –COOR′, in the molecule.

MATERIALS AND METHODS

Chemicals

L-Amino acids were esterified with appropriate alcohols by the thionyl chloride method [12–14]. The amino acid to be esterified was dissolved or suspended in the chosen alcohol and cooled to 263 K. Thionyl chloride was added slowly, in small molar excess relative to the amino acid, over a period of 30 min. The reaction mixture was then allowed to warm up and was left at room temperature for 48 h. After this period the hydrochloric acid and excess of alcohol were removed in vacuo. The resulting precipitates, which sometimes occurred only when ethyl ether was added, were separated by filtration and purified by repeated crystallization from the mixture

methanol–ethyl ether. The identity of the compounds was confirmed by elemental analysis (performed on a Carlo–Erba instrument, model 1106).

Apparatus

The dynamic thermal analyses were carried out on an OD-103 derivatograph (Monicon) with α-Al_2O_3 as reference, in a dynamic atmosphere of N_2. The samples (50 mg) were analysed in a shallow platinum crucible [15]. Other operating conditions were as follows: heating rate, ca. 5 K min^{-1}, sensitivities of DTG, DTA and TG galvanometers, 0.1, 0.5 and 50 mg, respectively. The thermogravimetric analyses under quasi isothermal–isobaric conditions [16] were performed on a Q-1500 derivatograph (Monicon) with 100 mg samples placed in a special platinum labyrinth crucible. The samples were heated at a rate of ca. 3 K min^{-1}. The rate of mass loss was adjusted to 2 mg min^{-1}.

Calculations

The quantum chemistry calculations were carried out using the MOPAC version 4.0 program package for personal computers [17]. The geometry optimizations of glycine and L-alanine methyl esters and glycine ethyl ester, as well as their protonated forms and decomposition fragments, were performed by applying the semiempirical MINDO/3 [18], MNDO [19] and AM1 [20] methods. The starting geometries of these molecules were modelled on the basis of chemical intuition and the work of Schaefer et al. [21]. The examinations regarding geometry of the transition state for the thermal decomposition (in the saddle point) were carried out at the level of the AM1 method [22].

The electrostatic part of the crystal lattice energy of L-proline phenylmethyl ester hydrochloride was derived adopting Ewald method [23,24] for unsymmetrical multiple-atom ions [25]. The quantum chemistry calculations necessary for these evaluations were done at the level of the CNDO/2 [26,27], MNDO [19] and INDO [26–29] methods. All calculations were carried out on an IBM PC computer.

RESULTS AND DISCUSSION

General features of the thermal decomposition

Thermal analysis curves recorded under both dynamic and quasi-isothermal–isobaric conditions for three chosen compounds are shown in Figs. 1 and 2. To enable further discussion, the essential parameters characterizing the thermal behaviour of the compounds studied, derived from the thermal

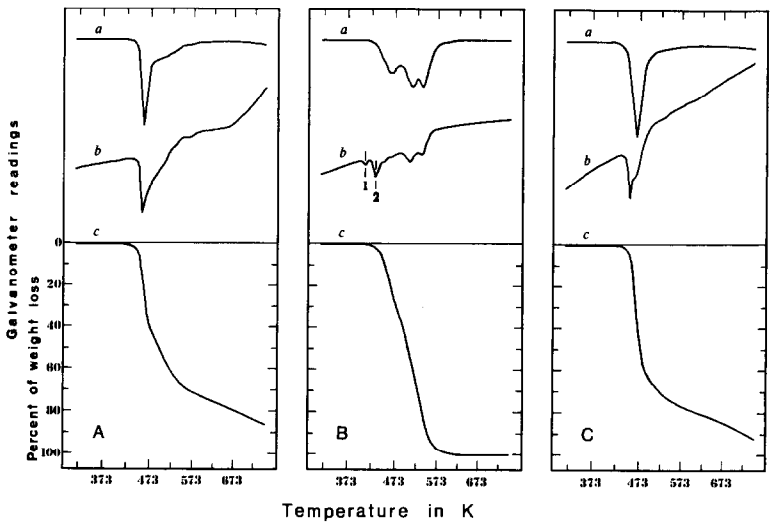

Fig. 1. Dynamic thermal analyses of hydrochlorides of glycine methyl ester (A), L-leucine methyl ester (B) and L-serine methyl ester (C). *a*, DTG; *b*, DTA; *c*, TG; 1, solid state phase transition; 2, melting.

analysis curves, are given in Table 1 together with the available information from the literature.

Thermal decomposition of all the compounds studied presents a multi-step pattern. The hydrochlorides of esters of L-valine, L-leucine and L-isoleucine undergo complete volatilization on heating up to 750 K. The remaining compounds studied undergo only partial volatilization with rising temperature. The solid residue formed at higher temperatures is presumably a mixture of carbonization products. The composition of neither gaseous nor solid products was examined in this work. The predictions regarding the

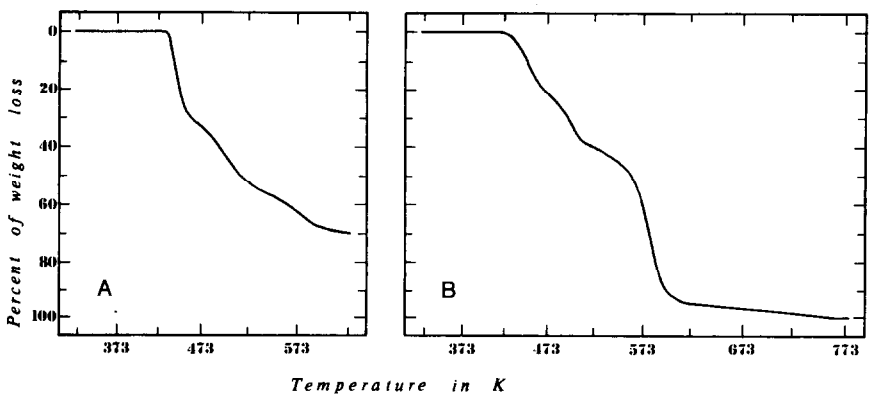

Fig. 2. TG analyses of hydrochlorides of glycine methyl ester (A) and L-leucine methyl ester (B) under quasi-isothermal–isobaric conditions.

possible pathways of thermolysis of these derivatives and thus reaction products will be presented subsequently. Nevertheless, some information regarding the nature of the thermal processes can be drawn from the thermoanalytical curves. Examining the data in Table 1 one notices that the temperatures of the onset of decomposition vary roughly within 70 K for the various compounds studied. The first (in the temperature scale) thermal process is accompanied by mass loss of the sample and is always of endothermic nature. Exothermic processes occur sometimes at higher temperatures, presumably with the participation of oxygen from the gaseous environment. Traces of oxygen are always present in the reaction zone owing to leaks in the derivatograph oven. These facts seem to indicate that the primary processes in the thermal decomposition of the compounds studied are mostly of endothermic nature and lead to products which are partially volatile at the temperature of decomposition.

The hydrochloride of the methyl ester of L-leucine exhibits phase transition below the melting point. Some of the compounds studied melt before the onset of thermolysis. The fusion of others occurs simultaneously with the decomposition process. Thus, the fusion process is not always reflected on the DTA curves.

Any of the compounds studied have, so far, been examined by thermoanalytical methods. It would be interesting, however, to compare the thermal features of appropriate amino acids and their hydrochlorides, on the one hand, and chloride salts of alkanamines on the other. The temperatures of the thermal decomposition of hydrochlorides of amino acid esters, i.e. T_p (from DTA and DTG) and $T_{0.01}$ (Table 1), are lower by as much as 100 K than those characteristic of the parent amino acids or their hydrochlorides [73,74]. Also, the comparison of thermolysis temperatures of amino acids determined by other techniques [75,76] with those for hydrochlorides of amino acid esters (Table 1) indicate that the compounds studied begin to decompose at lower temperatures. A similar conclusion comes from the analysis of vapour pressures of amino acids (Table 2). These facts clearly demonstrate that hydrochlorides of amino acid esters are less temperature resistant than the parent amino acids or their hydrochlorides.

The characteristic temperatures of thermolysis of the compounds studied are very similar to those found for alkanaminium chlorides [3,79]. However, the latter derivatives volatilize smoothly in one step, whereas decomposition of hydrochlorides of amino acid esters proceeds in several steps (Table 1), similarly to thermolysis of the original amino acids [80–83]. On the other hand, hydrochlorides of 2-aminooxy acids and their esters [84] exhibit much lower thermal stability than the compounds studied.

Nature of the decomposition process

With the lack of information regarding thermolysis products, and taking into account that the thermal decomposition of the compounds studied

TABLE 1

Thermal characteristics of hydrochlorides of 2-amino acid esters $[RCH(NH_2)COOR'] \cdot n HCl$

No. [a]	Amino acid (symbol)	R	R′	Temperature (K) and character of peaks in: [b,c]					Temperature (K) of onset of decomposition $T_{0.01}$ [b]
				DTG	DTA				
					Exo	Endo			
					T_p	T_o	T_m		T_p	
							This work [d]	From the literature [e]		
1	Glycine (Gly)	H	CH_3	456s, sh			(446–448)	448 [31] 448–449 [32]	454s, sh 570w	428 437(Q)
2	L-Alanine (L-Ala)	H_3C	CH_3	467w 547s, b	579m, b 763m, b		392 (381–383)	381 [33] 382–384 [34]	494w 529s, b	
3	L-Valine (L-Val)	$(H_3C)_2HC$	CH_3	468m, b 539s, sh			429(D) (433–435)	419–422 [35] 434–435 [36] 441 [37] 443 [38,39] 448 [40]	508m 538s, sh	418
			$C(CH_3)_3$	429s, sh 539s, sh			420(D)		428m, w 515, 534s, b	411
			$CH_2(C_6H_5)$	438s, sh 528, 536s, sh			426(D)	410–411 [41] 412–414 [42]	436m, sh 522s, b	414
4	L-Leucine (L-Leu)	$(H_3C)_2HCH_2C$	CH_3	460m, b 510, 539s, b		404	427(D) (423–425)	411–413 [43] 419–421 [30] 424–425 [44]	502m 535m	422 426(Q)
			$CH_2(C_6H_5)$	486, 531s, b			413	400–401 [45] 401 [46] 402 [47] 417–418 [41]	488, 525m, b	428
5	L-Isoleucine (L-Ileu)	$H_3CH_2CH(CH_3)C$	CH_3	457m, b 533s, sh			379 (372–374)	374 [48]	454m, b 534s, sh	409
6	L-Phenyl-alanine (L-Phe)	$(H_5C_6)H_2C$	CH_3	464m, b 524, 542s, b 627m, b	626m, b		(431–433)	432–433 [49] 432–434 [50] 433 [39,51]	444m, sh 510m, b	438

			CH_2CH_3	508s, b 611m, b	593m, b	434		495m, b 551m, b	441
			$C(CH_3)_3$	471s, sh 527, 543m, b 535m, b			(D) [52,53]	473m, sh 524, 544s, b 573w	444
			$CH_2(C_6H_5)$	478s, sh 504, 517m, b 553s, b 620m, b	609s, b		475 [13,41] 476 [46]	474s, sh 499w 545m, b	458
7	L-Serine (L-Ser)	$(HO)H_2C$	CH_3	464s, sh		(437–439)	427–428 [54] 438–439 [55] 440 [56] 441 [57]	448, 460m, b	431 426(Q)
8	L-Tyrosine (L-Tyr)	$[(p\text{–}HO)H_4C_6]H_2C$	CH_3	476m, sh 554m, sh		(461–463)	462–463 [12,30] 463 [58,59] 464–465 [50]	468m, sh 554m, sh	464
9 *	L-Lysine (L-Lys)	$(H_2N)H_2C(H_2C)_3$	CH_3	488m, sh 586s, b		(483–485)	476–478 [30] 485 [60]	489s, sh 583s, b	478
10 *	L-Arginine (L-Arg)	$(H_2N)CHN(H_2C)_3$ ‖ NH	CH_3	472m, sh 553m, b 614s, b		(467–469)	468 [61] 469 [40,62]	471s, sh 539m, b 601s, b	458
11 *	L-Histidine (L-His)	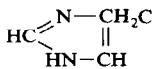	CH_3	479m, sh 541m, b 595m, b		(472–474)	470 [63] 470–472 [64] 473–474 [65]	477s, sh 531m, b 585m, sh	465
12	L-Tryptophan (L-Trp)	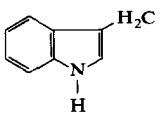	CH_3	493m, sh 551m, b 636m, b	629m, b	(485–487)	487 [66,67] 489(D) [40]	491m, sh 545m, b	476
13	L-Aspartic acid (L-Asp)	$(H_3CO_2C)H_2C$	H	481s, sh 650m, sh		473(D) (463–465)	464–466(D) [50] 477(D) [68]	483s, sh 651s, b	436
			CH_3	470s, b 641m, b		400		475s, b 652m, b	424
14	L-Glutamic acid (L-Glu)	$(H_3CO_2C)H_2CH_2C$	H	467s, b 558m, b		425(D)	434 [58] 445 [69]	466s, b 548m, b	411

TABLE 1 (continued)

No. [a]	Amino acid (symbol)	R	R′	Temperature (K) and character of peaks in: [b,c] DTG	DTA Exo T_p	DTA Endo T_o	DTA Endo T_m This work [d]	DTA Endo T_m From the literature [e]	DTA Endo T_p	Temperature (K) of onset of decomposition $T_{0.01}$ [b]
15	L-Proline [f] (L-Pro)	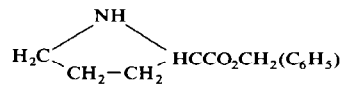		542s, sh			424(D)	421–422 [12,70]	537m, b	417
16	L-Methionine (L-Met)	$H_3CSCH_2CH_2C$	CH_3	481s, b 611m, b			418(D) (421–423)	420–423 [30] 423 [71]	479s, b	403
17	Creatine [g] (Cre)	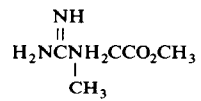		431s, sh 541m, b			425(D)	412–413 [72]	431m, sh 538s, sh	413

[a] Numbers without an asterisk represent monohydrochlorides ($n = 1$); those with an asterisk correspond to dihydrochlorides ($n = 2$).

[b] The symbols were taken from ref. 30. T_p, temperature of peak; T_o temperature of solid phase transition, T_m, temperature of melting, and $T_{0.01}$, temperature of onset of decomposition (i.e., temperature at which fraction reacted is equal to 0.01); (Q) indicates $T_{0.01}$ values determined from quasi-isothermal–isobaric measurements.

[c] w, Weak; m, medium; s, strong; sh, sharp; b, broad.

[d] The melting point determined using a standard capillary method is given in parentheses; (D) denotes melting with decomposition.

[e] References are given in square brackets.

[f] L-Proline phenylmethyl ester.

[g] Creatine methyl ester; creatine = *N*-(aminoiminomethyl)-*N*-methylglycine.III

TABLE 2

Enthalpies of formation and thermochemistry of the thermal decomposition of hydrochlorides of amino acid methyl esters [a]

Parent amino acid (see Table 1)	$\Delta H_{f,g}^{\ominus}$	$\Delta H_{f,c}^{\ominus}$	Thermodynamics of decomposition							
			$\Delta H_r^{\ominus}$ for reaction pathway				Volatilization temperature [b]			
							Parent amino acid [c]		Amine hydrochloride [d]	
			(I)	(II)	(III)	(III′)	$T_{0.01}$	T_v	$T_{0.01}$	T_v
Glycine	−371	−639	−70	−16	34	34	524 *	614 *	406 $^{+}$	514 $^{+}$
							533 **	632 **	410 $^{++}$	512 $^{++}$
L-Alanine	−445	−712	−32	25	41	98	518 *	605 *	416 $^{+}$	520 $^{+}$
									410 $^{++}$	512 $^{++}$
L-Valine	−434	−702		−33	−11	37	496 *	562 *	410 $^{++}$	512 $^{++}$
L-Leucine	−466	−733		−25		49	510 *	587 *	410 $^{++}$	512 $^{++}$
L-Isoleucine	−497	−764		8		80			410 $^{++}$	512 $^{++}$
L-Phenylalanine	−292	−559				59	524 *	603 *	410 $^{++}$	512 $^{++}$
L-Serine	−595	−863		31		97			410 $^{++}$	512 $^{++}$
L-Proline	−345	−613					534 *	678 *		

[a] $\Delta H_{f,g}^{\ominus} = \Delta H_{f,g}^{\ominus}[RCH(NH_2)COOR']$; $\Delta H_{f,c}^{\ominus} = \Delta H_{f,c}^{\ominus}[RCH(NH_2)COOR' \cdot HCl]$; $\Delta H_r^{\ominus}$, enthalpy of reaction; all enthalpy values (in kJ mol^{-1}) correspond to 298 K.

[b] Temperature values (in K) were evaluated using the van't Hoff equation: $n \ln(P/P_0) = -\Delta H_v/(RT) + \Delta H_v/(RT_v)$, where ΔH_v is the heat of volatilization, P is the vapour pressure at a given temperature T, P_0 represents the atmospheric pressure, R denotes the gas constant, T_v is the volatilization temperature, i.e., the temperature at which P attains P_0, and n accounts for the number of moles of gaseous molecules released from 1 mole of the solid substance ($n = 1$ for amino acids and $n = 2$ for hydrochlorides of amines); $T_{0.01}$ corresponds to $P/P_0 = 0.01$.

[c] Values calculated on the basis of the data on the volatilization of amino acids from ref. 77 (*) and ref. 78 (**).

[d] Calculated on the basis of the data on the volatilization of amine hydrochlorides from refs. 3 and 79; values correspond to the hydrochlorides of amines formed upon decomposition according to the first reaction pathway ($^{+}$) and second reaction pathway ($^{++}$).

presents a multi-step pattern, it is rather difficult to predict a priori all possible reaction pathways. A helpful feature in this case may be the knowledge of the thermal processes occurring upon heating of parent amino acids. It has been revealed that amino acids fairly easily undergo decarboxylation, leading to the corresponding amines [85–88]. This procedure has been even recommended as a preparative one [85]. Detailed analysis of the thermal decomposition products of glycine revealed the presence of large amounts of H_2O, CO_2 and NH_3 and traces of HCN and CH_3NH_2 among the volatile products [86]. The residue after pyrolysis of glycine appeared to be a mixture of polymeric substance and carbonization products [86]. Water, CO_2, appropriate amines and nitriles have also been reported as gaseous products of the thermolysis of other amino acids [85–87]. Moreover, the formation of unsaturated hydrocarbons and CO can be expected upon

pyrolysis of amino acids [74]. The structure of the compounds studied differs somewhat from that characteristic of the parent amino acids. Nevertheless, the thermal decomposition pathways can be expected to be similar in the case of both groups of compounds.

Preliminary insight into reaction dynamics can be obtained by analysing bond orders of all the bonds in the molecule. The values of this quantity are related to the strength of the bond and thus to bond energy. Therefore, bond order values provide qualitative information on the susceptibility of bonds to cleavage. In molecules of the compounds studied, the $\geq$N–H $\cdots$ Cl hydrogen bond, typical of hydrochlorides of amines, exhibits specific character, and it may be thought that it does not affect the destruction of the skeleton of a molecule. As is revealed by thermoanalytical data for amine hydrochlorides [3,79], this bond is selectively broken upon heating, with release of free amines and HCl. It can be thus assumed that the information regarding the thermal behaviour of amino acid ester molecules in the gaseous phase is representative for molecules of appropriate hydrochlorides in the solid phase. For none of the amino acid esters studied is the complete information regarding bond orders available. Therefore, we used the MOPAC

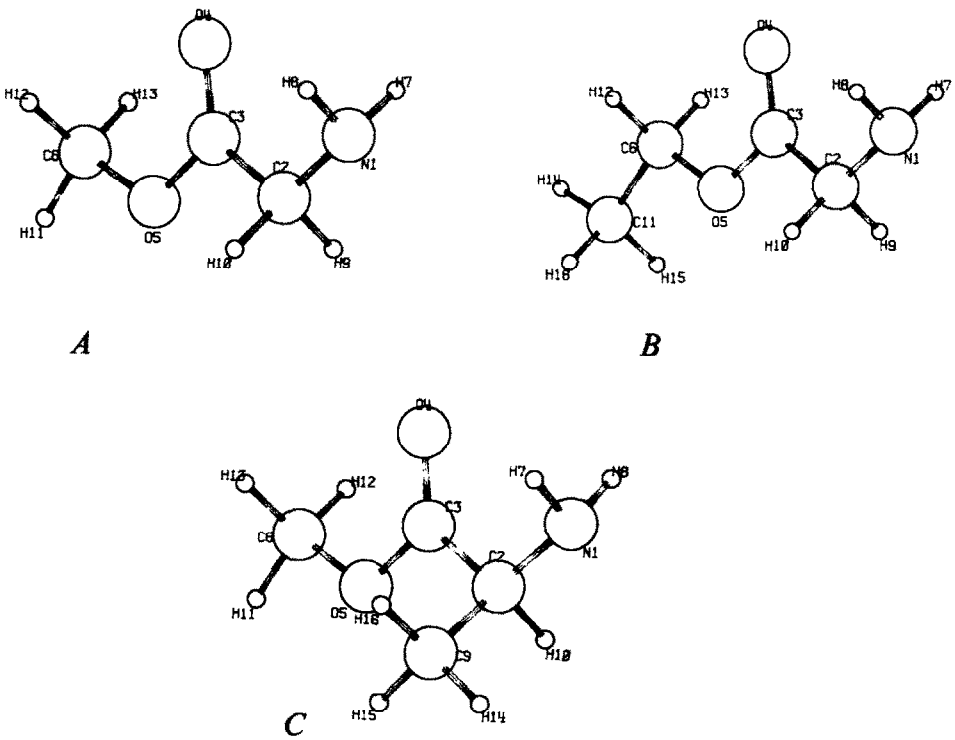

Fig. 3. The AM1 lowest energy structures of glycine methyl ester (*A*), glycine ethyl ester (*B*) and L-alanine methyl ester (*C*).

program package to calculate these data for three molecules chosen as examples, namely: glycine methyl ester, glycine ethyl ester and L-alanine methyl ester. Figure 3 shows the bonding geometry of these compounds, whereas Table 3 comprises appropriate bond order values. Analysing data in Table 3, one notices that the C2–C3 and O5–C6 bonds are the weakest in the molecules, and it could be thought that these bonds are broken first upon thermal decomposition of amino acid esters. The cleavage of even a single bond to form two radical species usually requires provision of the molecule with a relatively large amount of energy. In such a case thermal processes would be realized at quite high temperatures. Since the observed decomposition temperatures are rather low, it may be thought that destruction of the molecules proceeds exclusively by elimination of smaller molecular fragments. Such reaction pathways would, of course, require a suitable initial arrangement of the parent molecule and transfer to products though certain transition states. We will discuss this subject subsequently.

Just on the basis of chemical intuition, several pathways for the decomposition of amino acid esters can be predicted. They are shown below in eqns. (1)–(13).

	Reaction Pathway	
$RCH(NH_2)COOCH_2R'$		
$\rightarrow CO_2 + RCH(NH_2)CH_2R'$	I	(1)
$\rightarrow CO_2 + NH_3 + RCHCHR'$	II	(2)
$\rightarrow H_2 + CO_2 + RCN + CH_3R'$	III	(3)
$\rightarrow H_2 + CO_2 + HCN + RCH_2R'$	III′	(4)
$\rightarrow H_2 + RCN + R'CH_2COOH$	IV	(5)
$\rightarrow H_2 + HCN + R'CH_2COOR$	IV′	(6)
$\rightarrow CO + RCH_2NH_2 + R'CHO$	V	(7)
$\rightarrow H_2 + CO + RCN + R'CH_2OH$	VI	(8)
$\rightarrow H_2 + CO + HCN + R'CH_2OR$	VI′	(9)
$\rightarrow H_2 + RCN + HCHO + R'CHO$	VII	(10)
$\rightarrow H_2 + HCN + RCHO + R'CHO$	VII′	(11)
$\rightarrow CO_2 + RCH_2NH_2 + R'(alkene)$	VIII	(12)
$\rightarrow RCH(NH_2)COOH + R(alkene)$	IX	(13)

The above presented reaction pathways comprise possible molecular elimination mechanisms. They consider simple processes, e.g. those given by reaction (1), (2) or (13), which most probably proceed according to the unimolecular mechanism. Other, more complicated processes leading to

TABLE 3

Bond orders in molecules of amino acid esters

Glycine methyl ester		Glycine ethyl ester		L-alanine methyl ester	
Bond [a]	Bond order [b]	Bond [a]	Bond order [b]	Bond [a]	Bond order [b]
N1–C2	1.04	N1–C2	1.04	N1–C2	1.02
N1–H7	0.95	N1–H7	0.95	N1–H7	0.95
H1–H8	0.95	N1–H8	0.95	N1–H8	0.95
C2–C3	*0.88*	C2–C3	*0.88*	C2–C3	*0.87*
C2–H9	0.94	C2–H9	0.94	C2–C9	0.97
C2–H10	0.94	C2–H10	0.94	C2–H10	0.94
C3–O4	1.79	C3–O4	1.79	C3–O4	1.80
C3–O5	1.03	C3–O5	1.04	C3–O5	1.03
O5–C6	*0.95*	O5–C6	*0.93*	O5–C6	*0.95*
C6–H11	0.96	C6–C11	0.99	C6–H11	0.96
C6–H12	0.96	C6–H12	0.96	C6–H12	0.96
C6–H13	0.96	C6–H13	0.96	C6–H13	0.96
		C11–H14	0.97	C9–H14	0.97
		C11–H15	0.97	C9–H15	0.97
		C11–H16	0.97	C9–H16	0.97

[a] For numbering of atoms see Fig. 3.

[b] Values in italics are those for bonds broken upon decarboxylation.

three or more products can well be realized via several steps with different activation barriers.

Thermodynamics of the decomposition process

The primary information on the probability for a given reaction pathway is provided by thermochemical considerations. Unfortunately, none of the heats of formation of amino acid esters or their hydrochlorides is available. Therefore, we estimated heats of formation ($\Delta H_f^{\ominus}$) of some gaseous amino acid methyl esters by modifying heats of formation of gaseous amino acids reported in ref. 89 on the framework of the Benson group additivity method [90]. The necessary group parameter corresponding to the esterification of the carboxylic group was estimated by analysing differences in the heats of formation of carboxylic acids and their corresponding methyl esters. Similarly, values of $\Delta H_f^{\ominus}$ for L-isoleucine and L-serine were evaluated. These estimated enthalpies of formation of chosen amino acid esters are listed in Table 2. Values for the enthalpy of formation of crystalline hydrochlorides were estimated from a thermochemical cycle analogous to that for ammonium and alkanaminium chlorides [79], assuming for $\Delta H_{f,g}^{\ominus}$[HCl] a value equal to -92.3 kJ mol^{-1} [91,92], and for the heat of sublimation a value equal to 175 kJ mol^{-1} [84]. These latter values are also shown in Table 2. Using the thus derived enthalpies of formation of gaseous amino acid esters

and available literature values of the enthalpy of formation of decomposition products [89,91,92], we evaluated enthalpy changes for reaction pathways I, II and III (III'). These derived values are shown in Table 2.

To gather further information on the systems studied, we considered in detail the reaction pathways for the decomposition of glycine methyl ester, glycine ethyl ester and L-alanine methyl ester. Thermolysis of the above mentioned derivatives is demonstrated with eqns. (14)–(40) shown in Table 4. Table 4 also contains information on the enthalpy changes (ΔH_r) for appropriate reactions. The enthalpy changes were evaluated either on the basis of the experimental enthalpies of formation of the reaction products (Table 6) and estimated enthalpies of formation of substrates (Table 2) or using the enthalpies of formation of all reactants evaluated by the quantum chemistry methods MINDO/3, MNDO and AM1 (see Tables 5 and 6). The ΔH_r values indicate that decarboxylation via reaction pathway I is thermodynamically the most probable process. Decarboxylation according to mechanism II is also thermodynamically favourable. Decarboxylation via I or II leads to appropriate amines or NH_3. Both these products form hydrochlorides, similarly to the parent molecules. Thus, the thermodynamics of these two processes should be analogous for both free amino acids esters in the gaseous phase and their chloride salts in the solid phase. Amines are, furthermore, expected following decarboxylation via mechanism V. The process requires, however, a marked thermodynamic barrier to be overcome. Products containing an amine group can be also formed via mechanisms VIII and IX. The latter two pathways are feasible only when the esterified carboxylic group contains substituents more complex than methyl. The thermolysis according to reaction pathways III, IV, VI and VII should lead to derivatives containing the –CN group. Since such compounds do not exhibit basic character, they do not form chloride salts in the solid phase. It means that during decomposition via III, IV, VI and VII, accompanied by the evolution of gaseous products, an additional thermodynamic barrier over that resulting from the thermolysis of gaseous esters (Table 4) has to be overcome. This barrier, equal roughly to 175 kJ mol^{-1} (see text, above), is necessary to destroy the $\gtrless$N–H $\cdots$ Cl hydrogen bond and to transfer the amine and HCl released to the gaseous phase.

Mechanism of decarboxylation

No mechanistic considerations have so far been conducted for the compounds studied. In order to shed more light on this problem we analysed the decarboxylation of glycine methyl ester via reaction pathway I. For this purpose we used an opportunity which provided the MOPAC 4.0 program package [17]. This program enables optimization of the geometry of a molecule in the transition state (saddle point). Moreover, it provides several characteristics for a parent molecule, the molecule in the transition state and

TABLE 4

Enthalpies of the thermal decomposition (ΔH_r) of glycine methyl ester, glycine ethyl ester and L-alanine methyl ester, for various reaction pathways, evaluated using theoretical or experimental thermochemical data

Reaction pathway			ΔH_r (kJ mol^{-1})			
No.	Chemical expression	Eqn. No.	Theoretical [a]			Experimental [b]
			MINDO/3	MNDO	AM1	
I	$CH_2(NH_2)CO_2CH_3$					
	$\rightarrow CO_2 + CH_3CH_2NH_2$	(14)	−63.8	−1.9	0.3	−69.6
II	$\rightarrow CO_2 + NH_3 + CH_2CH_2$	(15)	44.3	92.9	102.1	−15.8
III	$\rightarrow H_2 + CO_2 + HCN + CH_4$	(16)	120.9	155.6	135.1	33.9
IV	$\rightarrow H_2 + HCN + CH_3CO_2H$	(17)	100.4	96.7	74.9	69.0
V	$\rightarrow CO + HCHO + CH_3NH_2$	(18)	219.9	175.2	211.2	129.2
VI	$\rightarrow H_2 + CO + HCN + CH_3OH$	(19)	279.3	255.0	243.4	189.8
VII	$\rightarrow H_2 + HCN + 2\,HCHO$	(20)	333.8	244.6	242.1	284.6
I	$CH_2(NH_2)CO_2CH_2CH_3$					
	$\rightarrow CO_2 + CH_3CH_2CH_2NH_2$	(21)	−31.8	1.0	−4.3	−57.6
II	$\rightarrow CO_2 + NH_3 + CH_3CHCH_2$	(22)	45.3	72.2	85.4	−13.5
III	$\rightarrow H_2 + CO_2 + HCN + CH_3CH_3$	(23)	119.3	145.3	123.3	59.3
IV	$\rightarrow H_2 + HCN + CH_3CH_2CO_2H$	(24)	128.9	99.9	73.8	83.1
V	$\rightarrow CO + CH_3CHO + CH_3NH_2$	(25)	200.5	158.8	193.7	106.5
VI	$\rightarrow H_2 + CO + HCN + CH_3CH_2OH$	(26)	282.9	255.1	237.8	190.9
VII	$\rightarrow H_2 + HCN + HCHO + CH_3CHO$	(27)	314.4	228.2	224.6	261.9
VIII	$\rightarrow CO_2 + CH_2CH_2 + CH_3NH_2$	(28)	118.4	110.1	126.1	42.1
IX	$\rightarrow CH_2(NH_2)CO_2H + CH_2CH_2$	(29)	106.4	55.5	66.2	73.3
I	$CH_3CH(NH_2)CO_2CH_3$					
	$\rightarrow CO_2 + CH_3CH(NH_2)CH_3$	(30)	−60.8	−2.5	−2.4	−32.2
II	$\rightarrow CO_2 + NH_3 + CH_3CHCH_2$	(31)	4.3	60.9	75.0	25.5
III	$\rightarrow H_2 + CO_2 + CH_4 + CH_3CN$	(32)	30.8	99.2	100.0	41.5
III′	$\rightarrow H_2 + CO_2 + HCN + CH_3CH_3$	(33)	78.3	134.0	112.9	98.2
IV	$\rightarrow H_2 + CH_3CN + CH_3CO_2H$	(34)	10.3	40.3	39.8	76.6
IV′	$\rightarrow H_2 + HCN + CH_3CO_2CH_3$	(35)	144.7	138.8	116.4	163.6
V	$\rightarrow CO + HCHO + CH_3CH_2NH_2$	(36)	187.5	160.8	192.7	178.6
VI	$\rightarrow H_2 + CO + CH_3OH + CH_3CN$	(37)	189.2	198.6	208.3	197.4
VI′	$\rightarrow H_2 + CO + HCN + CH_3OCH_3$	(38)	326.7	291.6	273.6	280.9
VII	$\rightarrow H_2 + 2\,HCHO + CH_3CN$	(39)	243.7	188.2	207.0	292.2
VII′	$\rightarrow H_2 + HCN + HCHO + CH_3CHO$	(40)	273.4	216.9	214.2	300.8

[a] Evaluated using enthalpies of formation of reactants from Tables 5 and 6.

[b] Calculated on the basis of the experimental and estimated enthalpies of formation of reactants shown in Tables 2 and 6.

reaction products. We performed these calculations at the level of the AM1 method. The initial structure of glycine methyl ester for these calculations was modelled starting from the lowest energy conformation obtained after AM1 geometry optimization (see Fig. 3). This structure is characterised by

the fact that fragments containing C(2) and C(6) atoms are situated *trans* relative to the C(3)–O(5) bond. The initial structure for saddle point calculations was such that four atoms, i.e. C(2), C(3), O(5) and C(6), were placed in a plane such that the C(6) atom was the shortest possible distance from C(2). The geometry of a conglomerate of the reaction products (i.e. geometry of the final stage of the reaction) was modelled by combining ethanamine and CO_2 molecules in the conformations appropriate for the unimolecular decomposition process. This geometry follows the idea that the CO_2 fragment moves out from the glycine methyl ester molecule thus allowing the remaining two fragments to form an ethanamine molecule. The structure of the molecule in the transition state, obtained after gradient minimization in the saddle point, is demonstrated in Fig. 4. To enable detailed comparison of the geometry of a parent molecule with that in the transition state we present in Table 7 the Z matrix for both species. It may be easily noticed that the transition state is characterized by longer C(2)–C(3) (change from 1.52 to 2.07 Å) and O(5)–C(6) (change from 1.43 to 2.20 Å) bonds, shorter C(3)–O(5) bond (change from 1.36 to 1.23 Å) and much shorter C(2)–C(6) distance (2.56 Å) than in the parent molecule. Among numerous parameters which the program provides for the molecule in the transition state, the most interesting is the enthalpy of formation. In our case, the value of this quantity is equal to 170.3 kJ mol^{-1}. If thermolysis were to proceed via a simple unimolecular step, the difference between this latter value and the value of the heat of formation of glycine methyl ester (Table 5) could be interpreted as a kinetic activation barrier for the process (ΔH_a). This difference is, however, equal to 568.1 kJ mol^{-1} and exceeds markedly the energy of simple single bonds, e.g. C–C, C–H, C–O or O–H. Therefore, if it was actually required to overcome such a barrier, it would be easier for the molecule to dissociate to radical fragments. The examination of many processes revealed that radical dissociation takes place in much

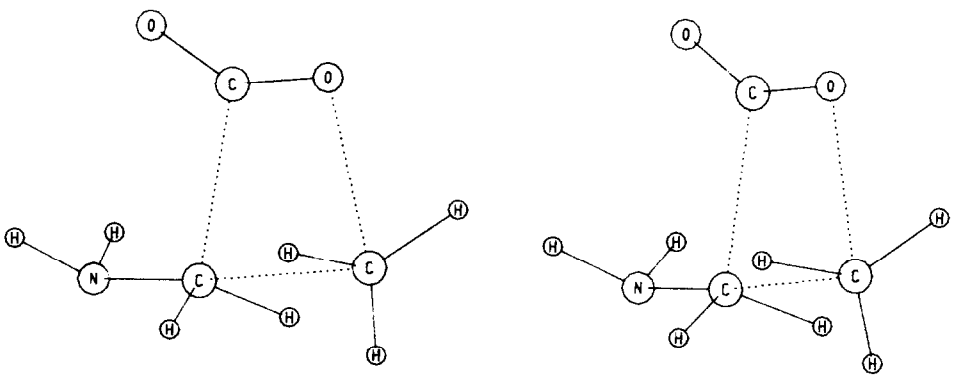

Fig. 4. The stereoview of the AM1 optimized transition state for the unimolecular decomposition of glycine methyl ester to CO_2 and ethanamine.

TABLE 5

Physicochemical characteristics for glycine methyl ester, glycine ethyl ester and L-alanine

Molecule	Heat of formation $\Delta H^{\ominus}_{f,298}$ (kJ mol^{-1})			Proton affinity [a] PA (kJ mol^{-1})			
	MINDO/3	MNDO	AM1	MINDO/3	MNDO	AM1	Experimental [93]
$CH_2(NH_2)CO_2CH_3$	−402.7	−367.9	−397.8	877	806	854	907
$CH_2(NH_2)CO_2CH_2CH_3$	−457.9	−390.1	−422.2	886	808	858	
$CH_3CH(NH_2)CO_2CH_3$	−416.9	−378.8	−411.8	890	815	872	
$CH_2(NH_3)CO_2CH_3^+$	256.5	362.8	284.7				
$CH_2(NH_3)CO_2CH_2CH_3^+$	192.5	338.0	256.0				
$CH_3CH(NH_3)CO_2CH_3^+$	229.0	342.9	252.6				

[a] For $\Delta H^{\ominus}_{f,g}[H^+]$, a value equal to 1536.2 kJ mol^{-1} [91,92] was used.

higher temperatures than those characterizing thermal decomposition of the compounds studied. It seems, therefore, that the enthalpy of formation of a molecule in the transition state is overestimated. Such a high ΔH_a value could be only feasible if decarboxylation of glycine methyl ester were to be realized through several consecutive steps. Then the energy barrier for the rate determining step would be expected to be lower than ΔH_a. Despite the fact that the predicted kinetic barrier cannot be accepted without some reservations, the geometry remains in accord with chemical intuition and our imagination on the structural transformations accompanying unimolecular decomposition.

Crystal lattice energy

A very important characteristic of solid substances is the crystal lattice energy. This quantity determines the magnitude of cohesive forces keeping molecules in the rigid solid phase. The chloride salts of nitrogen organic bases form ionic crystals similar to those characteristic of typical inorganic salts [94–96]. However, these substances differ from each other due to the fact that the former compounds contain highly unsymmetrical cations. In ionic crystals the main contribution to the crystal lattice energy is afforded by electrostatic interactions. Thus, we made an attempt to evaluate the energy of these interactions following an approach used for simple ionic crystals.

The lattice energy E_c of an ionic substance K_mA_n, defined as an energy change for the process

$$K_mA_n(c) \rightarrow mK^{\alpha n+}(g) + nA^{\alpha m-}(g) \qquad (41)$$

methyl ester and their protonated forms in the gaseous phase

Dipole moment (Debye)			Energies (eV) of					
			LUMO			HOMO		
MINDO/3	MNDO	AM1	MINDO/3	MNDO	AM1	MINDO/3	MNDO	AM1
1.19	1.33	1.16	0.80	0.74	0.98	−9.2	−10.8	−10.3
1.55	1.50	1.41	0.82	0.78	1.03	−9.1	−10.8	−10.3
1.34	1.47	1.38	0.79	0.78	1.03	−9.2	−10.8	−10.3
			−5.26	−4.87	−4.74	−15.2	−15.7	−15.5
			−5.13	−4.83	−4.66	−14.8	−15.4	−14.8
			−5.03	−4.74	−4.54	−15.0	−15.7	−15.4

TABLE 6

Theoretical and experimental heats of formation of expected gaseous thermal decomposition products of glycine methyl ester, glycine ethyl ester and L-alanine methyl ester

Compound	$\Delta H_{f,298}^{\ominus}$ (kJ mol^{-1})			
	Theoretical			Experimental [89,91,92]
	MINDO/3	MNDO	AM1	
H_2	0.5	3.0	−21.7	0
CO	−56.5	−24.8	−23.8	−110.5
CO_2	−400.6	−314.2	−334.1	−393.5
HCN	144.6	148.9	129.8	130.5
NH_3	−38.2	−25.3	−30.5	−46.1
H_2CO	−107.0	−137.6	−131.9	−108.6
CH_4	−26.3	−50.0	−36.7	−74.4
CH_2CH_2	80.4	64.5	68.9	52.5
CH_3OH	−212.0	−240.0	−238.7	−201.5
CH_3CN	40.3	81.6	80.7	64.3
CH_3CHO	−181.6	−176.2	−173.8	−166.1
CH_3NH_2	−19.3	−30.3	−30.9	−23.0
CH_3CH_3	−83.1	−82.5	−72.9	−83.8
CH_3CHCH_2	26.2	21.6	27.8	20.0
CH_3CH_2OH	−263.6	−262.1	−268.7	−235.2
$CH_3CH_2NH_2$	−65.9	−55.6	−63.4	−47.4
$CH_3CH_2CH_2NH_2$	−89.1	−74.9	−92.4	−70.2
$CH_3CH(NH_2)CH_3$	−77.1	−67.1	−80.1	−83.8
CH_3COOH	−447.4	−423.1	−431.0	−432.8
CH_3CH_2COOH	−474.1	−442.1	−456.5	−453.5
$CH_2(NH_2)COOH$	−431.9	−399.1	−424.9	−392.1
CH_3OCH_3	−178.8	−214.3	−222.5	−184.1
CH_3COOCH_3	−417.3	−391.9	−403.5	−411.9

TABLE 7

Z matrix of the isolated glycine methyl ester molecule and molecule of the compound in the transition state for unimolecular decomposition

Atom (Fig. 3)		Bond length (Å)	Bond angle (deg)	Dihedral angle (deg)	Connectivity chain		
No.	Symbol						
Glycine methyl ester molecule							
1	N	–	–	–	–	–	–
2	C	1.432	–	–	1	–	–
3	C	1.516	115.49	–	2	1	–
4	O	1.233	128.29	0.08	3	2	1
5	O	1.365	113.03	180.03	3	2	1
6	C	1.429	116.75	179.85	5	3	2
7	H	1.001	111.42	−60.97	1	2	3
8	H	1.001	111.40	60.93	1	2	3
9	H	1.128	107.39	−121.98	2	3	4
10	H	1.128	107.39	122.07	2	3	4
11	H	1.118	103.69	180.03	6	5	3
12	H	1.116	109.93	−60.57	6	5	3
13	H	1.116	109.92	60.64	6	5	3
Transition state molecule							
1	N	–	–	–	–	–	–
2	C	1.409	–	–	1	–	–
3	C	2.069	100.88	–	2	1	–
4	O	1.207	108.24	1.97	3	2	1
5	O	1.226	104.85	−178.44	3	2	1
6	C	2.199	110.53	−11.87	5	3	2
7	H	1.003	111.76	−63.29	1	2	3
8	H	1.003	111.83	58.47	1	2	3
9	H	1.107	109.33	119.31	2	1	3
10	H	1.106	111.37	−110.86	2	1	3
11	H	1.098	72.63	160.60	6	5	3
12	H	1.094	122.12	48.49	6	5	3
13	H	1.093	88.22	−77.89	6	5	3

(where α is the multiplier accounting for the actual valence of both ions), can be generally expressed with the equation [97–99]

$$E_c = -E_{el} + E_r - E_d + E_0 \tag{42}$$

where E_{el} is the term accounting for the electrostatic interactions between ions, E_r represents the repulsive interactions, E_d the van der Waals interactions and E_0 the zero point energy. Since terms E_r and E_d are roughly equal to each other, but have the opposite sign, and the E_0 term is not significant, the term describing electrostatic interactions well approximates the crystal lattice energy of ionic substances [97,99].

The electrostatic energy of 1 mol of ionic substance composed of structural units $(K^{\alpha n+})_m(A^{\alpha m-})_n$ (corresponding to the simplest formula unit of the molecule) is given by

$$E_{el} = 0.5N_A\left[mV^{(\alpha n+)} + nV^{(\alpha m-)}\right] \tag{43}$$

where N_A is Avogadro's number, whereas the factor of 0.5 eliminates the double counting of electrostatic interactions. $V^{(\alpha n+)}$ and $V^{(\alpha m-)}$ represent the potential energy of a single cation and anion, respectively, as a result of their interactions with all other ions. The mathematical expressions for these latter two quantities result from Coulomb's law and are

$$V^{(\alpha n+)} = \left[(\alpha n+)e^2/4\pi\epsilon_0 R_0\right]\sum_i z_i/\rho_{\alpha n+,i} \tag{44}$$

$$V^{(\alpha m-)} = \left[(\alpha m-)e^2/4\pi\epsilon_0 R_0\right]\sum_i z_i/\rho_{\alpha m-,i} \tag{45}$$

In eqns. (44) and (45) e denotes the absolute electron charge, ϵ_0 is the permittivity of free space, R_0 represents a unit of length on the molecular level (usually this quantity is equal to the shortest cation–anion distance or distance between other two characteristic points in the lattice; sometimes it is related to the dimensions of the unit cell), z_i represents relative charges of all other ions interacting with the cation (of relative charge $\alpha n+$) and anion (of relative charge $\alpha m-$) and $\rho_{\alpha n+,i}$ and $\rho_{\alpha m-,i}$ denote distances in the crystal from a given ion ($\alpha n+$ or $\alpha m-$) to the ion i, expressed in R_0 units (real distance $= \rho R_0$).

Combining eqns. (43)–(45) one obtains an equation often recommended for the evaluation of the electrostatic energy of ionic crystals, namely

$$E_{el} = aM/R_0 \tag{46}$$

where a is a constant equal to

$$a = N_A(\alpha n+)(\alpha m-)e^2/4\pi\epsilon_0 \tag{47}$$

and M is the Madelung constant

$$M = 0.5\sum_i\left[m(z_i/\alpha m-)/\rho_{\alpha n+,i} + n(z_i/\alpha n+)/\rho_{\alpha m-,i}\right] \tag{48}$$

The Madelung constant is always positive and depends on the type of a lattice. On the other hand, constant a is always negative because of the opposite signs of $(\alpha n+)$ and $(\alpha m-)$. Therefore, E_{el} is also negative, and this is in accord with the fact that electrostatic interactions cause stabilization of ions in the lattice. The value of constant a is easy to obtain for a given substance. The real problem, however, consists in calculation of the Madelung constant. The well known method for the evaluation of E_{el}, and thus M, has been developed by Ewald [23] and subsequently generalized by Bertaut [24]. The method utilizes the effect of periodical location of charged atoms in the lattice. It further admits that each point charge exhibits

Gaussian distribution. Combining the above facts and introducing Fourier transformation, Ewald derived an expression for the electrostatic energy which contains two quickly converging infinite series. This expression can easily be solved numerically.

To evaluate the Madelung constant and thus E_{el}, the complete crystal structure has to be known. Among the compounds examined, X-ray studies have been undertaken for hydrochlorides of glycine ethyl ester [100] and L-proline phenylmethyl ester [101]. However, only the structural data for the latter compound enable the evaluation of E_{el}. X-ray studies on L-proline phenylmethyl ester hydrochloride provide the positions in the lattice of C, N, O and Cl atoms. Taking the skeleton of the compound thus established, the positions of H atoms in the lattice have been found by geometry optimization using the MNDO method. In calculations of E_{el} values we assumed that a single negative charge is localized on the Cl atom. The charge distribution between all the atoms of the singly protonated L-proline phenylmethyl ester molecule was found by applying CNDO/2, MNDO and INDO methods (Table 8). This distribution corresponds to the isolated

TABLE 8

Crystal lattice energy (in kJ mol^{-1}) of hydrochlorides of amino acid esters

Substance	E_c values evaluated using eqn. (49)				Calculated by Ewald method
	MINDO /3 [a]	MNDO [b]	AM1 [c]	Others	
$CH_2(NH_2)COOCH_3 \cdot HCl$	688	759	711	658 [d]	
$CH_2(NH_2)COOCH_2CH_3 \cdot HCl$	679	757	707	–	
$CH_3CH(NH_2)COOCH_3 \cdot HCl$	675	750	693	–	
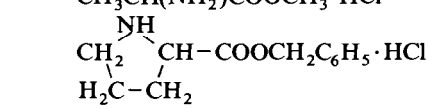					
				651 [e]	432 [f]
					439 [g]
					461 [h]
					428 [i]
					432 [j]

[a] PA values from MINDO/3 calculations (Table 5).
[b] PA values from MNDO calculations (Table 5).
[c] PA values from AM1 calculations (Table 5).
[d] PA value from ref. 93 (Table 5).
[e] PA value for ester was assumed to be the same as for L-Proline (i.e. 914 kJ mol^{-1}). The latter was taken from ref. 102.
[f] Charge distribution calculated by CNDO/2 method.
[g] Charge distribution calculated by CNDO/2 method with deorthogonalized orbitals.
[h] Charge distribution calculated by MNDO method.
[i] Charge distribution calculated by INDO method.
[j] Charge distribution calculated by INDO method with deorthogonalized orbitals.

cation. Providing, initially, all the atoms in the lattice with point charges are found in the above described manner, the electrostatic energy of hydrochloride of L-proline phenylmethyl ester was derived using the previously adopted program for the Ewald method [25]. This information is compiled in Table 8.

To enable the comparison of calculated values of electrostatic energy for the hydrochloride of L-proline phenylmethyl ester, we estimated the value of E_c for the compound on the basis of a thermochemical cycle which is analogous to that for alkanaminium chlorides [79]. From this cycle the following equation can be derived

$$E_c = \Delta H_v + \Delta H_{f,g}[H^+] + \Delta H_{r,g}[Cl^-] - \Delta H_{f,g}[HCl] - PA - 2RT \qquad (49)$$

In eqn. (49) all magnitudes refer to $T = 298$ K and 1 atmosphere; R denotes the gas constant; ΔH_v is the enthalpy of volatilization of the hydrochloride of amino acid ester (taken to be 175 kJ mol^{-1}—see text above); PA is the proton affinity of the amino acid ester; $\Delta H_{f,g}[H^+] = 1536.2$ kJ mol^{-1} [91,92]; $\Delta H_{f,g}[Cl^-] = -233.2$ kJ mol^{-1} [91,92]; and $\Delta H_{f,g}[HCl] = -92.3$ kJ mol^{-1} [91,92].

The proton affinity of L-proline phenylmethyl ester is not known, although a value of PA is known for L-proline [102]. The work of Locke and McIver [93] has shown that proton affinity values do not differ markedly for amino acids and their esters. Therefore, we assumed the value of PA for L-proline phenylmethyl ester to be the same as for the parent amino acid. The value of E_c derived with this assumption for the hydrochloride of L-proline phenylmethyl ester is shown in Table 8. As may be noticed, the estimated E_c value is much higher than the E_{el} values determined theoretically. At present, we are unable to account for this discrepancy. Using eqn. (49) and taking proton affinities for glycine methyl and ethyl esters and L-alanine methyl ester from Table 5, we also estimated crystal lattice energies of hydrochlorides of the latter three amino acid esters. It is interesting that values of crystal lattice energy derived in different and independent ways do not vary from each other markedly for the three analysed compounds. This trend is analogous to that observed in the series of chloride salts of numerous nitrogen organic bases [3–5,79]. It is also worth mentioning that numerical values of E_c for hydrochlorides of amino acid esters (Table 8) are very similar to those for chloride salts of numerous nitrogen organic bases [3–5,79]. This fact may suggest that cohesive forces have the same origin in both groups of compounds.

Physicochemical characteristics derived by quantum chemistry methods

The semiempirical quantum chemistry methods MINDO/3, MNDO and AM1 enabled the evaluation of heats of formation of several chemical species, their dipole moments and energies of LUMO (lowest unoccupied molecular orbital) and HOMO (highest occupied molecular orbital) orbitals.

The derived heats of formation were compared, where possible, with the experimental ones (Table 6). As one may note, the agreement is not always satisfactory, particularly in the case of small molecules. It is perhaps worth mentioning that it is generally recognized that the AM1 method best reproduces experimental thermochemical data [20]. The heats of formation of glycine methyl ester, glycine ethyl ester and L-alanine methyl ester and of their protonated forms are shown in Table 5. To our knowledge no thermochemical data for the latter compounds have so far been reported. The calculated heats of formation of the monoprotonated forms enable also the evaluation of proton affinities for the corresponding free bases (B). This can be done using the equation

$$PA[B] = \Delta H_{f,g}^{\ominus}[B] - \Delta H_{f,g}^{\ominus}[BH^+] + \Delta H_{f,g}^{\ominus}[H^+] \quad (50)$$

in which all values correspond to 298 K. Since the MINDO/3 [103], MNDO [104] and AM1 [105] methods reproduce rather poorly the heat of formation of the proton, we used experimental values of $\Delta H_{f,g}^{\ominus}[H^+]$ (Table 5) for the evaluation of PA values. These are also shown in Table 5. All three quantum chemistry methods applied predict somewhat lower values of PA for glycine methyl ester than that found experimentally.

Table 5 also shows the values of three other quantities, namely dipole moments in the gaseous phase and energies of LUMO and HOMO orbitals. The latter quantities can be related to the redox properties of the compounds examined. The energy of the HOMO orbital represents the ionization potential of the molecule.

CONCLUDING REMARKS

The thermal features of hydrochlorides of numerous naturally occurring amino acid esters examined in this work extend our knowledge on the behaviour of this very important group of nitrogen organic bases. Thermoanalytical studies revealed that, in the temperature range in which hydrochlorides of amines undergo only simple volatilization [3–5,79], the hydrochlorides of amino acid esters undergo complex chemical changes. This means that amino acid esters are less thermally stable than similar amines.

The examination of the thermodynamics of possible decomposition pathways suggests that the most feasible processes are those leading to the decarboxylation of the parent molecules. The analysis of the dynamics of the decarboxylation process, performed at the level of AM1 method using glycine methyl ester molecule as an example, suggests that the process proceeds through a four centre transition state. The structure of the decomposing molecule in the transition state seems to fit well to our ideas on the mechanism of chemical processes. However, the difference between the derived enthalpy of formation of the molecule in the saddle point and the

enthalpy of formation of the lowest energy structure of the parent molecule is too high to represent the kinetic activation barrier for the process. Nevertheless, the study on the decomposition dynamics brings nearer our understanding of the mechanism of this particular process.

Insight into the nature of cohesive forces keeping molecules of hydrochlorides of amino acid esters in the solid phase and determining their properties has been obtained by analysing lattice energy problems. The very important finding resulting from these examinations is that the theoretically calculated electrostatic energy corresponds reasonably to the crystal lattice energy estimated from the thermochemical cycle. Furthermore, the crystal lattice energy of hydrochlorides of amines [3–5,79] and amino acid esters (Table 8) are close to each other in magnitude. This means that cohesive forces in both groups of compounds have the same origin. It should be also mentioned that the $\geq N-H \cdots Cl$ hydrogen bond, which may be expected to play a predominant role in the solid state interactions, occurs in both groups of compounds. Therefore the differences in the thermal behaviour of chloride salts of amines and amino acid esters are a consequence of differences in the nature of other sites in the molecules.

REFERENCES

1 M. Eckert and G. Zundel, J. Phys. Chem., 91 (1987) 5170.
2 G. Zundel, J. Mol. Struct., 177 (1988) 43.
3 J. Błażejowski and E. Kowalewska, Thermochim. Acta, 105 (1986) 257.
4 J. Łubkowski and J. Błażejowski, J. Chem. Soc., Faraday Trans. 1, 82 (1986) 3069.
5 J. Łubkowski and J. Błażejowski, Thermochim. Acta, 121 (1987) 413.
6 J. Łubkowski and J. Błażejowski, Thermochim. Acta, 157 (1990) 259.
7 P. Dokurno, J. Łubkowski and J. Błażejowski, Thermochim. Acta, 165 (1990) 31.
8 T. Janiak and J. Błażejowski, Thermochim. Acta, 141 (1989) 93.
9 T. Janiak and J. Błażejowski, Thermochim. Acta, 156 (1989) 27.
10 T. Janiak and J. Błażejowski, Thermochim. Acta, 157 (1990) 137.
11 J. Błażejowski, J. Szychliński and E. Kowalewska, Thermochim. Acta, 108 (1986) 239.
12 M. Brenner and E. Huber, Helv. Chim. Acta, 36 (1953) 1109.
13 J. Ramachandran and C.H. Li, J. Org. Chem., 28 (1963) 173.
14 R.P. Patel and S. Price, J. Org. Chem., 30 (1965) 3775.
15 J. Paulik, F. Paulik and L. Erdey, Anal. Chim. Acta, 34 (1966) 419.
16 J. Paulik and F. Paulik, Comprehensive Analytical Chemistry, Vol. 12, Part A, Elsevier, Amsterdam, 1981, p. 47.
17 The Quantum Chemistry Program Exchange (QCPE; Program No. QCMP019), Indiana University, Department of Chemistry, Bloomington, IN.
18 R.C. Bingham, M.J.S. Dewar and D.H. Lo, J. Am. Chem. Soc., 97 (1975) 1285, 1294, 1302, 1307.
19 M.J.S. Dewar and W. Thiel, J. Am. Chem. Soc., 99 (1977) 4899, 4907.
20 M.J.S. Dewar, E.G. Zoebisch, E.F. Healy and J.J.P. Stewart, J. Am. Chem. Soc., 107 (1985) 3902.
21 L. Schaefer, C. van Alsenoy, J.N. Scarsdale, V.J. Klimkowski and J.D. Ewbank, J. Comput. Chem., 2 (1981) 410.

22 M.J.S. Dewar, E.F. Healy and J.J.P. Stewart, J. Chem. Soc., Faraday Trans. 2, 80 (1984) 227.
23 P.P. Ewald, Ann. Phys. (Leipzig), 64 (1921) 253.
24 E.F. Bertaut, J. Phys. Radium (Paris), 13 (1952) 499.
25 J. Łubkowski and J. Błażejowski, J. Therm. Anal., in press.
26 J.A. Pople and D.L. Beveridge, Approximate Molecular Orbital Theory, McGraw-Hill, New York, 1970.
27 J.A. Pople and G.A. Segal, J. Chem. Phys., 43 (1965) 136; 44 (1966) 3289.
28 J.A. Pople, D.L. Beveridge and P.A. Dobosh, J. Chem. Phys., 47 (1967) 2026.
29 R.N. Dixon, Mol. Phys., 12 (1967) 83.
30 R.C. Mackenzie, J. Therm. Anal., 21 (1981) 173.
31 J.R. Rachele, J. Org. Chem., 28 (1963) 2898.
32 T. Curtius and F. Goebel, J. Prakt. Chem., 37 (1888) 150.
33 H. Zahn and H. Schussler, Justus Liebigs Ann. Chem., 641 (1961) 176.
34 W. Grassmann, E. Wunsch and A. Riedel, Chem. Ber., 91 (1958) 455.
35 S.R.L.M. Synge, Biochem. J., 42 (1948) 99.
36 D.A. Rowlands and G.T. Young, J. Chem. Soc., (1952) 3937.
37 E.L. Smith, D.H. Spackmann and W.J. Polglase, J. Biol. Chem., 199 (1952) 804.
38 J.I. Harris and T.S. Work, Biochem. J., 46 (1950) 196.
39 R.A. Boissonnas, S. Guttmann, P.-A. Jaquenoud and J.-P. Waller, Helv. Chim. Acta, 39 (1956) 1421.
40 R.A. Boissonnas, S. Guttmann, R.L. Huguenin, P.-A. Jaquenoud and E. Sandrin, Helv. Chim. Acta, 41 (1958) 1867.
41 Y. Iwakura, K. Hagashi, S. Kang and K. Nakaoji, Bull. Chem. Soc. Jpn., 37 (1964) 1707.
42 K. Inouye and H. Otsuda, Bull. Chem. Soc. Jpn., 34 (1961) 4.
43 F. Weygand and W. Swodenk, Chem. Ber., 93 (1960) 1693.
44 M.A. Nyman and R.M. Herbst, J. Org. Chem., 15 (1950) 108.
45 R. Krug and K. Nowak, Rocz. Chem., 39 (1965) 1343.
46 B.F. Erlanger and R.M. Hall, J. Am. Chem. Soc., 76 (1954) 5781.
47 H.K. Miller and H. Waelsch, J. Am. Chem. Soc., 74 (1952) 1092.
48 C. Ressler and V. du Vigneaud, J. Am. Chem. Soc., 79 (1957) 4511.
49 A.W. Schrecker and J.L. Hartwell, J. Am. Chem. Soc., 79 (1957) 3827.
50 H. Schwarz, F.M. Bumpus and I.H. Page, J. Am. Chem. Soc., 79 (1957) 5697.
51 A. Fontana and E. Scoftone, Gazz. Chim. Ital., 98 (1968) 1261.
52 R.W. Roeske, Chem. Ind., (1959) 1121.
53 A. Vollmar and M.S. Dunn, J. Org. Chem., 25 (1960) 387.
54 J.A. Maclaren, W.E. Savige and J.M. Swan, Aust. J. Chem., 11 (1958) 345.
55 J.I. Harris and J.S. Fruton, J. Biol. Chem., 191 (1951) 193.
56 E. Fischer, Chem. Ber., 39 (1906) 2949.
57 S. Guttmann and R.A. Boissonnas, Helv. Chim. Acta, 41 (1958) 1852.
58 R.A. Boissonnas, S. Guttmann, P.-A. Jaquenoud and J.-P. Waller, Helv. Chim. Acta, 38 (1955) 1491.
59 E. Wunsch, G. Fries and A. Zwick, Chem. Ber., 91 (1958) 542.
60 M. Bergmann, L. Zarvas and J.P. Greenstein, Chem. Ber., 65 (1932) 1692.
61 E. Fischer, Chem. Ber., 38 (1905) 4186.
62 J.P. Greenstein, M. Winitz, P. Gullino, S.M. Birnbaum and M.C. Otey, Arch. Biochem. Biophys., 64 (1956) 342.
63 V. Vigneaud and O.K. Behrens, J. Biol. Chem., 117 (1937) 27.
64 A.A. Glemzha and S.E. Severin, Izv. Akad. Nauk SSSR, Ser. Khim., (1966) 861.
65 N.C. Davis, J. Biol. Chem., 223 (1956) 935.
66 E. Abderhalden and M. Kempe, J. Physiol. Chem., 52 (1907) 207.
67 H. Peter, M. Brugger, J. Schreiber and A. Eschenmoser, Helv. Chim. Acta, 46 (1963) 577.

68 M. Goodman and F. Boardman, J. Am. Chem. Soc., 85 (1963) 2483.
69 J. Budnik, V. Kvita, J. Lukac and V. Mychajlyszyn, Czech, Patent 109, 835, Feb 1964, Chem. Abstr., 60 (1964) 15984a.
70 R.E. Neuman and E.L. Smith, J. Biol. Chem., 193 (1951) 97.
71 C.A. Dekker, S.P. Taylor and J.S. Fruton, J. Biol. Chem., 180 (1949) 155.
72 A.W. Dox and L. Yoder, J. Biol. Chem., 54 (1922) 671.
73 W.W. Wendlandt, Texas J. Sci., 12 (1960) 138.
74 S. Cantarini and W.W. Wendlandt, Thermochim. Acta, 70 (1983) 283.
75 J.W. Brown, Trans. R. Soc. Can., Sect. 3, 26 (1932) 173; Chem. Abstr., 27 (1933) 1617.
76 M.S. Dunn and T.W. Brophy. J. Biol. Chem., 99 (1932) 221.
77 S. Takagi, H. Chihara and S. Seki, Bull. Chem. Soc. Jpn., 32 (1959) 84.
78 H.J. Svec and D.D. Clyde, J. Chem. Eng. Data, 10 (1965) 151.
79 J. Błażejowski, Thermochim. Acta, 68 (1983) 233.
80 A.M. Bryan and P.G. Olafsson, Anal. Lett., 2 (1969) 505.
81 P.G. Olafsson and A.M. Bryan, Microchim. Acta, (1970) 871.
82 P.G. Olafsson and A.M. Bryan, Geochim. Cosmochim. Acta, 35 (1971) 337.
83 P.G. Olafsson and A.M. Bryan, Polym. Lett., 9 (1971) 521.
84 Z. Warnke and J. Błażejowski, Thermochim. Acta, 108 (1986) 265.
85 K. Dose, Chem. Ber., 90 (1957) 1251.
86 K. Heyns and K. Pavel, Z. Naturforsch. B, 12 (1957) 97, 109.
87 S.S. Mal, N.S. Volosovich and V.E. Rakovskii, Khim. Genezis Torfa Sapropelei, (1962) 93; Chem. Abstr., 58 (1963) 7760f.
88 M.N. Chumachenko and N.A. Khabarova, Sb. Tr. Vses. Zaochn. Politekh. Inst., (39) (1967) 5; Chem. Abstr., 69 (1968) 76323c.
89 J.B. Pedley, R.D. Naylor and S.P. Kirby, Thermochemical Data of Organic Compounds, Chapman and Hall, London, 2nd edn., 1986.
90 S.W. Benson, F.R. Cruickshank, D.M. Golden, G.R. Haugen, H.E. O'Neal, A.S. Rodgers, R. Shaw and R. Walsh, Chem. Rev., 69 (1969) 279.
91 K.P. Mishchenko and A.A. Ravdel, Kratki Spravochnik Fiziko, Khimicheskikh Velichin, Khimiya, Leningrad, 5th edn., 1967.
92 D.D. Wagman, W.H. Evans, V.B. Parker, R.H. Schumm, I. Halow, S.M. Bailey, K.L. Churney and R.L. Nuttall, J. Phys. Chem. Ref. Data, 11 (1982) Suppl. 2.
93 M.J. Locke and R.T. McIver, J. Am. Chem. Soc., 105 (1983) 4226.
94 J. Lindgren and I. Olovsson, Acta Crystallogr., Sect. B, 24 (1968) 549, 554.
95 S.T. Rao and M. Sundaralingam, Acta Crystallogr., Sect. B, 25 (1969) 2509.
96 M. Kurahashi, P. Engel and W. Nowacki, Z. Kristallogr., 152 (1980) 147.
97 K.P. Thakur, Aust. J. Phys., 29 (1976) 39.
98 H.D.B. Jenkins and K.F. Pratt, Adv. Inorg. Chem. Radiochem., 22 (1979) 1.
99 G. Raghurama and R. Narayan, J. Phys. Chem. Solids, 44 (1983) 633.
100 P.R. Narasimhan and G.D. Nigam, Z. Kristallogr., 141 (1975) 476.
101 M.E. Kamwaya, O. Oster and H. Bradaczek, Acta Crystallogr., Sect. B, 37 (1981) 1391.
102 M. Meot-Ner, E.P. Hunter and F.H. Field, J. Am. Chem. Soc., 101 (1979) 686.
103 W.L. Jorgensen, J. Am. Chem. Soc., 100 (1978) 1049, 1057.
104 S. Olivella, F. Urpi and J. Vilarrasa, J. Comput. Chem., 5 (1984) 230.
105 M.J.S. Dewar and K.M. Dieter, J. Am. Chem. Soc., 108 (1986) 8075.